GEOPHYSICAL RESEARCH LETTERS, VOL. 34, L23707, doi:10.1029/2007GL031826, 2007

Future regime shift in feedbacks during Arctic winter

James R. Miller,[1] Yonghua Chen,[2] Gary L. Russell,[3] and Jennifer A. Francis[1]

Received 27 August 2007; revised 21 October 2007; accepted 6 November 2007; published 8 December 2007.

[1] The Arctic is among the regions where climate is changing most rapidly today. Climate change is amplified by a variety of positive feedbacks, many of which are linked with changes in water vapor, cloud cover, and other cloud properties. We use a global climate model to examine several of these feedbacks, with a particular emphasis on determining whether there are significant temporal changes in these feedbacks that would make them stronger or weaker during the 21st century. The model results indicate that one of the significant positive feedbacks on Arctic surface air temperature in winter weakens substantially toward the end of the 21st century. The feedback loop begins with a temperature increase that produces increases in water vapor, cloud cover, and cloud optical depth which increase the downward longwave flux by 30 Wm^{-2} by 2060 which then increases the surface air temperature. **Citation:** Miller, J. R., Y. Chen, G. L. Russell, and J. A. Francis (2007), Future regime shift in feedbacks during Arctic winter, *Geophys. Res. Lett.*, *34*, L23707, doi:10.1029/2007GL031826.

1. Introduction

[2] Observed warming of the Arctic surface during recent decades is substantially larger than that in lower latitudes [e.g., *Serreze and Francis*, 2006], and global climate models project that this trend will continue. In addition to changes in temperature, other climate variables have also changed significantly during the past few decades [e.g., *Dickson*, 1999; *Serreze et al.*, 2007]. Change appears to be occurring on time scales associated with the North Atlantic Oscillation and on longer time scales likely related to increasing levels of atmospheric greenhouse gases [*Overland and Wang*, 2005]. During the past three decades, the extent of Arctic sea-ice has decreased [*Cavalieri et al.*, 2003; *Comiso*, 2006; *Stroeve et al.*, 2005] and sea-ice thickness has decreased by approximately 40% [*Rothrock et al.*, 1999]. *Belchansky et al.* [2004] find that the Arctic melt season has lengthened since 1979. *Francis and Hunter* [2007] examined possible linkages between declining perennial sea-ice and atmospheric forcing variables. Because of the short or sparse observation records, it is difficult to distinguish between the contributions to these trends by decadal variability and by increasing concentrations of anthropogenic greenhouse gases.

[3] The amplification of high-latitude climate change results from complex positive feedbacks involving exchanges of energy and water mass between the ocean, sea ice, and atmosphere. The positive feedback related to changes in sea-ice albedo is one of the most frequently mentioned, however there are other positive feedbacks that are also important. Among these are feedbacks related to water vapor and clouds. *Chen et al.* [2003, 2006] demonstrated the importance of correctly representing in climate models the relationships among Arctic cloud and radiative properties. The present paper examines how some of these relationships and feedbacks may change in simulations of future climate.

[4] We focus on the winter season at the site of the Surface Heat Budget of the Arctic (SHEBA) field campaign in the Beaufort Sea, north of Alaska from October 1997 through October 1998. A previous study by *Chen et al.* [2003] showed good agreement on the relationships between observed and modeled variables in this region. This site has extensive measurements of atmospheric and surface properties, and arguably the processes and conditions in the Beaufort Sea are the best known in the Arctic Ocean owing to this and other field campaigns. We examine the positive feedback in which a temperature increase leads to an increase in water vapor, cloud cover, and cloud optical depth, which increase the downward longwave flux (DLF) which subsequently increases the surface air temperature. The focus is on the link between DLF and water vapor and cloud properties during both present conditions and the 21st century. Section 2 provides a brief description of the climate model, and the results are given in section 3. Discussion and conclusions are presented in section 4.

2. Model Description

[5] The global climate model used in this study is based on, but modified from, the work by *Russell et al.* [1995]. Simulations from this model have been used by *Nakecenovic et al.* [2007]. Both the atmosphere and ocean use the C-grid numerical scheme of *Arakawa and Lamb* [1977] to solve the momentum equations. The model resolution is $3° \times 4°$ in latitude and longitude with 12 vertical layers in the atmosphere and up to 16 in the ocean. The atmosphere and ocean are coupled synchronously every hour. The atmospheric model uses *Russell and Lerner*'s [1981] linear upstream scheme to advect potential enthalpy and water vapor. All significant atmospheric gases and aerosols are used to calculate the radiative term. The ocean model based on the work by *Russell et al.* [1995] has a free surface, employs the linear upstream scheme for the advection of heat and salt, and uses the K-profile parameterization (KPP) of *Large et al.* [1994] for the vertical mixing. The model also calculates at each time step the flow of mass, potential enthalpy, and salt through 16 narrow (sub-grid scale) straits in response to

[1]Institute of Marine and Coastal Sciences, Rutgers, the State University of New Jersey, New Brunswick, New Jersey, USA.
[2]Department of Applied Physics and Applied Mathematics, Columbia University, New York, New York, USA.
[3]NASA Goddard Institute for Space Studies, New York, New York, USA.

0094-8276/07/2007GL031826$05.00

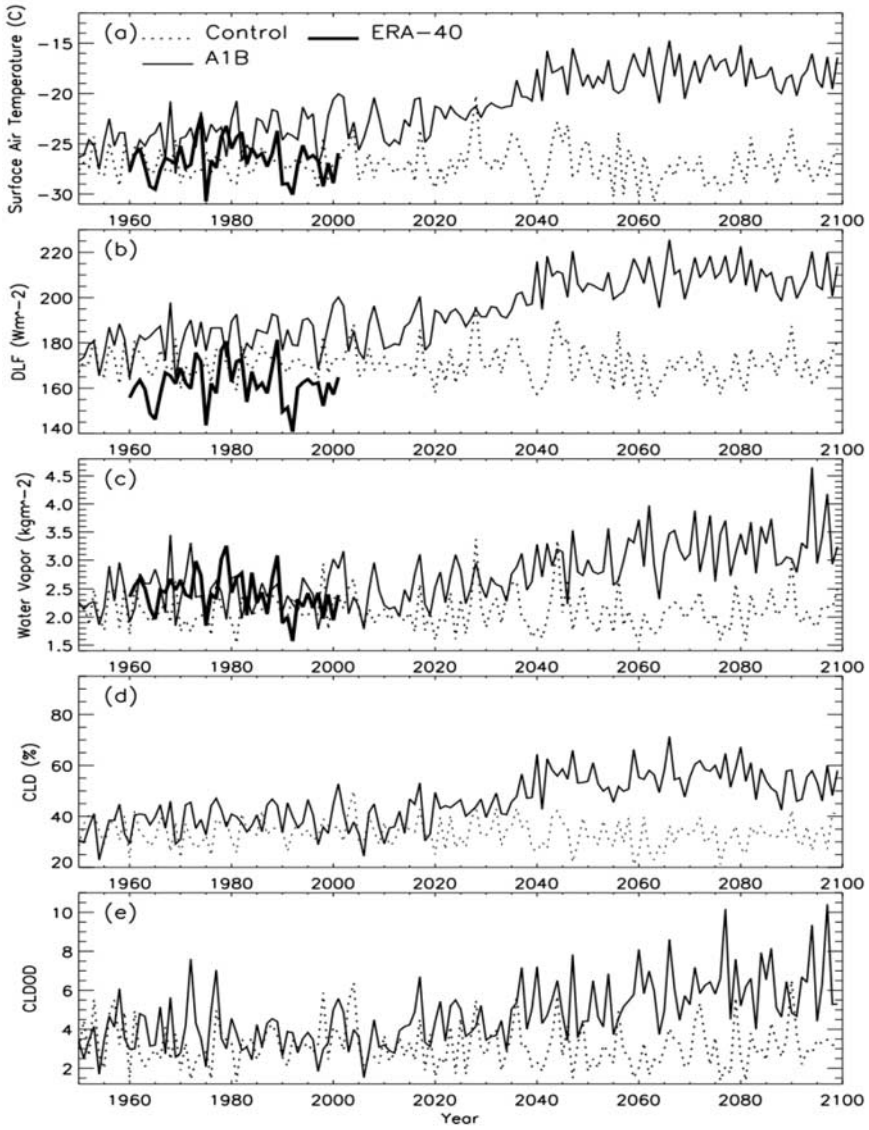

Figure 1. Climate variables for the control simulation and transient experiment (A1B) from 1950 to 2100 for (a) surface air temperature, (b) downward longwave flux (DLF), (c) atmospheric water vapor, (d) cloud cover (CLD), and (e) cloud optical depth (CLDOD). The ERA-40 observations for surface air temperature, DLF, and atmospheric water vapor are shown for the period from 1960 to 2000. The bold solid line represents ERA-40, the thin solid line is the A1B simulation and the dotted line is the control.

the oceanic pressure gradient between the grid cells on either end of the strait. Freshwater is added directly to the ocean by precipitation and river flow and is removed by evaporation. There is a four-layer thermodynamic sea-ice model, and sea-ice advection is based on the scheme described by *Miller and Russell* [1997]. River discharge is calculated directly as part of the model simulation according to the river routing scheme of *Miller et al.* [1994].

[6] Two model simulations were run from 1850 to 2100. The control simulation uses the same 1850 atmospheric composition for all years. The transient experiment includes observed greenhouse gases and estimates of tropospheric sulfate aerosols from 1850 to 2003, followed by projections of greenhouse gases and aerosols from 2004 to 2100 based on scenario A1B [*Nakecenovic et al.*, 2007], in which greenhouse gases increase at a moderate rate. It assumes rapid economic growth, a gradual decline in population after 2050, and that new technologies will increase energy efficiency. The changes in tropospheric sulfate aerosols through 2100 are based on *Pham et al.* [2005]. Model results are averaged over ten grid cells at the SHEBA site in the Beaufort Sea.

3. Results

[7] In this section we present modeled changes in winter surface air temperature, total-atmospheric water vapor, cloud properties, and downward longwave flux incident at the surface in several 20-year-periods during this century as concentrations of greenhouse gases continue to increase (Figure 1). Observed surface air temperature, atmospheric water vapor, and DLF obtained from the 40-year European Centre for Medium-Range Weather Forecasts (ECMWF) Reanalysis (ERA-40) are also presented for the end of the

Table 1. Relationships Between Modeled Downward Longwave Flux at the Surface and Three Other Climate Variables[a]

	Period		
Variable Pairs	1961–1980	2046–2065	2081–2100
DLF vs. water vapor (W kg^{-1})	19.83	13.31 (−33%)	12.37 (−7%)
DLF vs. cloud cover (W m^{-2} $\%^{-1}$)	0.82	0.74 (−10%)	0.74 (0%)
DLF vs. cloud optical depth (W m^{-2})	3.75	2.17 (−42%)	2.02 (−5%)

[a]DLF, downward longwave flux. Other climate variables are atmospheric water vapor, cloud cover, and cloud optical depth. These relationships are for an average over the SHEBA area in the Arctic Ocean from the transient experiment and represent the relationships for the three different 20-year periods shown. Values in parentheses are the changes in percentage from the previous 20-year period.

20th century. Surface air temperature at the SHEBA site (Figure 1a) increases steadily during the first half of the 21st century in the transient experiment, after which the warming stops. There is a similar trend in DLF (Figure 1b) at the surface during this period. Previous studies suggested that part of the enhanced wintertime warming during recent decades may have occurred in response to increased water vapor and cloud cover [*Miller and Russell*, 2002; *Wang and Key*, 2005]. Evidence supporting the roles of water vapor and cloud properties in contributing to the positive feedback on surface air temperature through DLF is provided by Figures 1c–1e. Increases in these quantities are most rapid during the first half of the century, while the rate of change in the second half is near zero. Although the focus of this study is on one model simulation rather than an ensemble mean, the results suggest that the climate system may enter a new stable regime that could last for decades, assuming that scenario A1B resembles reality.

[8] What factors contribute to the temporal changes in the variables in Figure 1? There are several possibilities: one is that temporal changes occur in the relationships between variables, which in turn lead to changes in the strength of the feedbacks. A positive feedback on surface air temperature results from the increase in DLF that occurs in response to increasing levels of atmospheric water vapor as the climate warms. As *Chen et al.* [2006] show, the relationship between some climate variables, such as longwave flux and water vapor, depends on the amount of water vapor initially present. One of the factors that makes the water vapor feedback so strong during the Arctic winter in the early years of the model simulation is that the mean concentration of water vapor is very low (2.2 kg m^{-2}, see Figure 1) and is in the range where DLF is most sensitive. Table 1 presents the sensitivities of pairs of climate variables. For each quantity, the differences from one day to the next for twenty winter seasons are averaged over the SHEBA site cells. The slope of 600 daily scatter plot values for DLF and another quantity are shown in Table 1. For the period between 1961 and 1980, DLF in the transient experiment increases by 19.83 W m^{-2} for each one kg m^{-2} increase in atmospheric water vapor. However, by the middle of the 21st century, the DLF increases by only 13.31 W kg^{-1}, because it becomes less sensitive to changes in water vapor as moisture content increases.

[9] Temporal changes in the relationships between DLF and increasing cloud cover and cloud optical depth are also evident in Table 1. As cloud cover and cloud optical depth increase during the 21st century, the sensitivity of DLF to changes in cloud cover is reduced by about 10% which is significantly smaller than that for water vapor, while the reduction in sensitivity to cloud optical depth (42%) is slightly larger than that for water vapor. We hypothesize that these reductions in the sensitivity of DLF to water vapor and cloud properties are at least partly responsible for the stabilization of temperature toward the end of the 21st century.

4. Discussion and Conclusions

[10] These results are consistent with previous studies [*Francis and Hunter*, 2007; *Miller and Russell*, 2002] that identified increasing DLF — due primarily to increasing water vapor, cloud cover and cloud optical depth – as playing an important role in the present-day Arctic system. Our findings are also consistent with other studies [*Chen et al.*, 2006] suggesting that the strength of these relationships may depend on the range of values of each climate variable during a specific period of time. In this study, we use a global climate model to examine several feedbacks on Arctic surface air temperature to investigate their behavior during the 21st century. The feedbacks are related to increases in downward longwave flux caused by increases in water vapor, cloud cover, and cloud optical depth, which occur as a consequence of increasing temperatures. The resultant increase in DLF leads to increased temperature in a positive feedback loop. The model results indicate that the enhanced Arctic wintertime warming slows toward the end of the 21st century, in part because of a regime shift in which the positive feedbacks weaken.

[11] Our results indicate that the sensitivity of DLF and surface air temperature to changes in water vapor and cloud optical depth is larger in the 20th century's drier and less cloudy atmosphere. The change in water vapor is responsible for a corresponding shift in the positive feedback on surface air temperature because additional increases in atmospheric water vapor that are induced by increases in temperature cause smaller increases in DLF than in the earlier regime with less water vapor. Hence, the positive feedback on surface air temperature weakens. The same regime shift occurs with increasing cloud optical depth, perhaps owing to an increase in liquid-containing clouds as the Arctic warms. Although this paper has not specifically examined the part of the feedback loop that produces the increase in atmospheric water vapor, this increase is consistent with modeled winter increases in open water and latent heat flux in the study region.

[12] Most of the increase in the variables shown in Figure 1 occurs between 2000 and 2040. Still uncertain is whether the 30 W m^{-2} increase in DLF during this period occurs primarily in response to increasing atmospheric water vapor or increases in cloud properties (i.e., cloud cover and cloud optical depth). Although we cannot answer this question definitively because increases in water vapor and cloud properties are not independent, a rough calculation using Figure 1 and Table 1 indicates that each contributes about equally.

[13] We recognize that these results may be specific to this model and the single realization that has been exam-

ined. In addition, the model's largest increases in cloud properties occur during the winter season, while observations indicate that the increases are strongest in the spring [*Francis and Hunter*, 2006; *Wang and Key*, 2005]. Because the mean water vapor is lowest during the winter season rather than in the spring, the results here are likely to overemphasize the potential changes in the feedback. As climate continues to change through this century, however, it is likely that the changes observed to date will extend to winter as well. An important issue that has not been discussed in this paper is that there can also be significant positive feedbacks between DLF and the climate variables discussed here that occur during the summer season. *Francis and Hunter* [2006] have found this to be the case in the recent climate record.

[14] **Acknowledgments.** We would like to acknowledge support for this study from NASA grant NAG5-11720. Partial support for J.R.M. was provided by Project 32103 of the New Jersey Agricultural Experiment Station. We are grateful to Elias Hunter for extracting the ERA-40 observations at SHEBA sites and to two anonymous reviewers.

References

Arakawa, A., and V. R. Lamb (1977), Computational design of the basic dynamical processes of the UCLA general circulation model, *Methods Comput. Phys.*, *17*, 174–267.

Belchansky, G. I., D. C. Douglas, and N. G. Platonov (2004), Duration of the Arctic sea ice melt season: Regional and interannual variability, 1979–2001, *J. Clim.*, *17*, 67–80.

Cavalieri, D. J., C. L. Parkinson, and K. Y. Vinnikov (2003), 30-Year satellite record reveals contrasting Arctic and Antarctic decadal sea ice variability, *Geophys. Res. Lett.*, *30*(18), 1970, doi:10.1029/2003GL018031.

Chen, Y., J. R. Miller, J. A. Francis, G. L. Russell, and F. Aires (2003), Observed and modeled relationships among Arctic climate variables, *J. Geophys. Res.*, *108*(D24), 4799, doi:10.1029/2003JD003824.

Chen, Y., F. Aires, J. A. Francis, and J. R. Miller (2006), Observed relationships between Arctic longwave cloud forcing and cloud parameters using a neural network, *J. Clim.*, *19*, 4087–4104.

Comiso, J. C. (2006), Arctic warming signals from satellite observations, *Weather*, *61*, 70–76.

Dickson, B. (1999), All change in the Arctic, *Nature*, *397*, 389–391.

Francis, J. A., and E. Hunter (2006), New insight into the disappearing Arctic sea ice, *Eos Trans. AGU*, *87*, 509.

Francis, J. A., and E. Hunter (2007), Change in the fabric of the Arctic greenhouse blanket, *Environ. Res. Lett*, in press.

Large, W. G., J. C. McWilliams, and S. C. Doney (1994), Oceanic vertical mixing: review and a model with non-local boundary layer parameterization, *Rev. Geophys.*, *32*, 363–403.

Miller, J. R., and G. L. Russell (1997), Investigating the interactions among river flow, salinity, and sea ice using a global coupled atmosphere-ocean-ice model, *Ann. Glaciol.*, *25*, 121–126.

Miller, J. R., and G. L. Russell (2002), Projected impact of climate change on the energy budget of the Arctic Ocean by a global climate model, *J. Clim.*, *15*, 3028–3042.

Miller, J. R., G. L. Russell, and G. Caliri (1994), Continental scale river flow in climate models, *J. Clim.*, *7*, 914–928.

Nakecenovic, N., et al. (2007), *Special Report on Emission Scenarios*, edited by N. Nakicenovic and R. Swart, Intergov. Panel on Clim. Change, Geneva, Switzerland. (Available at http://www.grida.no/climate/ipcc/emission/index.htm)

Overland, J. E., and M. Wang (2005), The Arctic climate paradox: The recent decrease of the Arctic Oscillation, *Geophys. Res. Lett.*, *32*, L06701, doi:10.1029/2004GL021752.

Pham, M., O. Boucher, and D. Hauglustaine (2005), Changes in atmospheric sulfur burdens and concentrations and resulting radiative forcings under IPCC SRES emission scenarios for 1990–2100, *J. Geophys. Res.*, *110*, D06112, doi:10.1029/2004JD005125.

Rothrock, D. A., Y. Yu, and G. A. Maykut (1999), Thinning of the Arctic sea-ice cover, *Geophys. Res. Lett.*, *26*, 3469–3472.

Russell, G. L., and J. A. Lerner (1981), A new finite differencing scheme for the tracer transport equation, *J. Appl. Meteorol.*, *20*, 1483–1498.

Russell, G. L., J. R. Miller, and D. Rind (1995), A coupled atmosphere-ocean model for transient climate change studies, *Atmos. Ocean*, *33*, 683–730.

Serreze, M. C., and J. A. Francis (2006), The Arctic amplification debate, *Clim. Change*, *76*, doi:10.1007/s10584-005-9017-y.

Serreze, M. C., M. M. Holland, and J. Stroeve (2007), Perspectives on the Arctic's shrinking sea-ice cover, *Science*, *315*, doi:10.1126/science.1139426.

Stroeve, J. C., M. C. Serreze, F. Fetterer, T. Arbetter, W. Meier, J. Maslanik, and K. Knowles (2005), Tracking the Arctic's shrinking ice cover: Another extreme September minimum in 2004, *Geophys. Res. Lett.*, *32*, L04501, doi:10.1029/2004GL021810.

Wang, X., and J. R. Key (2005), Arctic surface, cloud, and radiation properties based on the AVHRR Polar Pathfinder dataset. part II: Recent trends, *J. Clim.*, *18*, 2575–2593.

Y. Chen, Department of Applied Physics and Applied Mathematics, Columbia University, 200 S. W. Mudd Building, 500 W. 120th Street, New York, NY 10027, USA.

J. A. Francis and J. R. Miller, Institute of Marine and Coastal Sciences, Rutgers University, 71 Dudley Road, New Brunswick, NJ 08901, USA. (miller@marine.rutgers.edu)

G. L. Russell, NASA Goddard Institute for Space Studies, 2880 Broadway, New York, NY 10025, USA.